Institute of Paper Science and Technology
Atlanta, Georgia

IPST Technical Paper Series Number 782

Microstructural Disorder, Mesoscale Finite Elements, and Macroscopic Response

M. Ostoja-Starzewski

April 1999

Submitted to
Proceedings of the Royal Society, London—Series A

Copyright© 1999 by the Institute of Paper Science and Technology

For Members Only

INSTITUTE OF PAPER SCIENCE AND TECHNOLOGY
PURPOSE AND MISSIONS

The Institute of Paper Science and Technology is an independent graduate school, research organization, and information center for science and technology mainly concerned with manufacture and uses of pulp, paper, paperboard, and other forest products and byproducts. Established in 1929, the Institute provides research and information services to the wood, fiber, and allied industries in a unique partnership between education and business. The Institute is supported by 52 North American companies. The purpose of the Institute is fulfilled through four missions, which are:

- to provide a multidisciplinary education to students who advance the science and technology of the industry and who rise into leadership positions within the industry;
- to conduct and foster research that creates knowledge to satisfy the technological needs of the industry;
- to serve as a key global resource for the acquisition, assessment, and dissemination of industry information, providing critically important information to decision-makers at all levels of the industry; and
- to aggressively seek out technological opportunities and facilitate the transfer and implementation of those technologies in collaboration with industry partners.

ACCREDITATION

The Institute of Paper Science and Technology is accredited by the Commission on Colleges of the Southern Association of Colleges and Schools to award the Master of Science and Doctor of Philosophy degrees.

NOTICE AND DISCLAIMER

The Institute of Paper Science and Technology (IPST) has provided a high standard of professional service and has put forth its best efforts within the time and funds available for this project. The information and conclusions are advisory and are intended only for internal use by any company who may receive this report. Each company must decide for itself the best approach to solving any problems it may have and how, or whether, this reported information should be considered in its approach.

IPST does not recommend particular products, procedures, materials, or service. These are included only in the interest of completeness within a laboratory context and budgetary constraint. Actual products, procedures, materials, and services used may differ and are peculiar to the operations of each company.

In no event shall IPST or its employees and agents have any obligation or liability for damages including, but not limited to, consequential damages arising out of or in connection with any company's use of or inability to use the reported information. IPST provides no warranty or guaranty of results.

The Institute of Paper Science and Technology assures equal opportunity to all qualified persons without regard to race, color, religion, sex, national origin, age, disability, marital status, or Vietnam era veterans status in the admission to, participation in, treatment of, or employment in the programs and activities which the Institute operates.

Microstructural disorder, mesoscale finite elements, and macroscopic response

Martin Ostoja-Starzewski

Institute of Paper Science and Technology, and
Georgia Institute of Technology,
500 10th St., N.W., Atlanta, GA 30318-5794, U.S.A.

Abstract

Consideration of boundary value problems in mechanics of materials with disordered microstructures leads to the introduction of an intermediate scale - a mesoscale - which specifies the resolution of a finite element mesh relative to the microscale. The effective elastic mesoscale response is bounded by the Dirichlet and Neumann boundary value problems. The two estimates, separately, provide inputs to two finite element schemes - based on minimum potential and complementary energy principles, respectively - for bounding the global response. While in the classical case of a homogeneous material, these bounds are convergent with the finite elements becoming infinitesimal, the presence of a disordered, nonperiodic microstructure prevents such a convergence and leads to a possibility of an optimal mesoscale. The method is demonstrated on an example of torsion of a bar having a percolating two-phase microstructure of over a hundred thousand grains. By passing to an ensemble setting, we arrive at a hierarchy of two random continuum fields which provide input to a stochastic finite element method.

1. Introduction

Central to the entire field of continuum mechanics is the concept of a Representative Volume Element (RVE). It postulates the existence of a scale L of RVE much larger than the microscale d, which corresponds to characteristic size of a single grain in soil, fiber in a composite, crystal in a metal or ceramic, crack in a continuum, etc., Fig. 1. At the same time, L is required to be much smaller than the macroscopic dimensions and characteristic lengths L_{macro} of variation of global stress, strain and displacement fields

$$d < L \ll L_{macro} \tag{1.1}$$

Thus, fundamental issues concern (i) the dependence of effective moduli on L, and (ii) the setup of a finite element method for global response as L ceases to be infinitesimal relative to L_{macro}.

Indeed, the deterministic finite element methods strongly rely on the RVE concept in that every single finite element is larger than the length scales of fluctuation of the microstructure. This situation, however, is not the same in the so-called *stochastic finite elements* (SFE) which postulate the existence of some random fields of material properties with continuum realizations, and then, on that basis, set up the stiffness matrices (e.g, Benaroya & Rehak, 1988; Ghanem & Spanos, 1991; Ditlevsen, 1996). Typically, the SFE studies are concerned with linear elastic structural responses and depend on a straightforward randomization of Hooke's law, that is

$$\underset{\sim}{\sigma} = \underline{\underline{C}}(\underset{\sim}{x}, \omega)\underset{\sim}{\varepsilon} \tag{1.2}$$

In equation (1.2) $\underset{\sim}{x}$ stands for a location within the body domain, ω is an index from the sample space Ω, and $C(\underset{\sim}{x}, \omega)$ is a continuous realization of a random tensor field of stiffness. Implicit in the assumption (1.2) is the invertibility of such a constitutive law, that is

$$\underset{\sim}{\varepsilon} = S(\underset{\sim}{x}, \omega)\underset{\sim}{\sigma} \qquad S(\underset{\sim}{x}, \omega) = C^{-1}(\underset{\sim}{x}, \omega) \tag{1.3}$$

whereby $\underset{\sim}{\varepsilon}$ and $\underset{\sim}{\sigma}$ in (1.2) and $(1.3)_1$, respectively, are uniform fields applied to a hypothetical and

unspecified Representative Volume Element (RVE) of a random medium. In fact, in the conventional SFE studies, a locally isotropic form involving a random field of Young's modulus and Poisson's ratio is adopted. Then, various other assumptions are made: either both elastic constants are considered to be random fields - usually of a Gaussian type - or one of them is taken as a constant; correlations are exponential, etc. Summarizing, no connection to any microstructure is made in setting up of these random fields, and thus, in formulating the element and global stiffness matrices.

In this paper we outline a passage from the microstructure to a continuum approximation. This is done with the help of a *mesoscale window* which allows a rigorous definition of the effective properties - the larger the window, the weaker is the random scatter in these properties and the closer we are to the conventional macroscopic properties sought by classical micromechanics methods. On finite scales, the window's mesoscale response is non-unique as it depends on the type of loading imposed on its boundaries; also it is anisotropic. Since the window plays the role of a mesoscale finite element, this choice of boundary conditions has to be consistent with the variational principle employed for determination of the global response: Dirichlet conditions go with the minimum energy, while Neumann conditions go with the minimum complementary energy. Thus, two bounds on the global response are obtained with these principles; an exact solution, obtained by a computational micromechanics method, is shown to fall in between. We illustrate the entire procedure on an example of torsion of a bar having a percolating two-phase microstructure of Voronoi mosaic geometry with over one hundred thousand grains aligned with the bar's axis.

2. Mesoscale moduli and random fields

(a) A hierarchy of bounds

We address the issues posed in the introduction in the context of two-dimensional, two-phase microstructures of linear elastic materials governed locally by a Laplace equation. The microstructural geometry is specified by a Voronoi mosaic (generated from a Poisson point field). Each cell

of the mosaic is being occupied by either phase 1 or 2, according to a probability equal to the global volume fraction, which is chosen at 50% in Fig. 2. Since the Voronoi cells are six-connected on average, we have a percolating system which clearly lacks any periodicity.

The Hooke's law of either phase (1 or 2) is given by

$$\sigma_i = C_{ij}\varepsilon_j \qquad i,j = 1,2 \qquad C_{ij} = C^{(1)}\delta_{ij} \qquad or \qquad C^{(2)}\delta_{ij} \tag{2.1}$$

where, in the case of anti-plane shear, we denote

$$\sigma_i \equiv \sigma_{i3} \qquad \varepsilon_i \equiv \varepsilon_{i3} \qquad i,j = 1,2 \tag{2.2}$$

On the microscale, the governing equation of this piecewise-constant material is

$$C\left(\frac{\partial^2 u}{\partial x_1} + \frac{\partial^2 u}{\partial x_2}\right) = 0 \qquad C = C^{(1)} or C^{(2)} \qquad u \equiv u_3 \tag{2.3}$$

The isotropy of both stiffness tensors $C^{(1)}$ and $C^{(2)}$ in (2.1) leads to a *contrast* $\alpha \equiv C^{(2)}/C^{(1)}$. When $\alpha = 1$ the material is homogeneous, otherwise, heterogeneous. Figure 2 depicts one realization $\mathbf{B}(\omega)$ of a *random medium*, which, as is commonly done in mechanics of random media, is taken as a set $\boldsymbol{B} = \{\mathbf{B}(\omega);\ \omega \in \Omega\}$. The microstructure chosen here may be applied to model a range of different materials - examples are offered by duplex steels for a finite α (Werner *et al*, 1994), or porous materials for an extreme $\alpha = 0$ or ∞.

In the following, it will be useful to introduce a *window* of size L (e.g., Ostoja-Starzewski, 1993) and then work with a nondimensional parameter, relative to the grain size d, to be called a *mesoscale* $\delta = L/d$. To define the effective, in-plane moduli of a finite window domain of scale δ we choose an approach based on an interpretation of a Hooke's law as one in which either a uniform strain ε_j^0 or a uniform stress σ_j^0 is prescribed. In the first case, we should choose essential (Dirichlet) boundary conditions, while in the second case, we should choose natural (Neumann)

boundary conditions. The first setup is

$$\bar{\sigma}_i = C^e_{ij}\varepsilon^0_j \qquad under \qquad u(\underset{\sim}{x}) = \varepsilon^0_j L_j \qquad \forall \underset{\sim}{x} \in \partial \boldsymbol{B} \tag{2.4}$$

where $\bar{\sigma}_{ij}$ is the resulting mean (volume average) stress, and which leads to an effective stiffness $\boldsymbol{C}^e_\delta$. The second setup is

$$\bar{\varepsilon}_i = S^n_{ij}\sigma^0_j \qquad under \qquad t(\underset{\sim}{x}) = \sigma^0_j n_j(\underset{\sim}{x}) \qquad \forall \underset{\sim}{x} \in \partial \boldsymbol{B} \tag{2.5}$$

where $\bar{\varepsilon}_{ij}$ is the resulting mean (volume average) strain, and leads to an effective compliance $\boldsymbol{S}^n_\delta$. Determination of either second rank tensor, $\boldsymbol{C}^e_\delta$ or $\boldsymbol{S}^n_\delta$, requires three tests (for the 11-, 22-, and 12-components).

For any realization $\mathbf{B}(\omega)$, a window's response on the mesoscale (δ finite) is, under these definitions, nonunique - because $C^e_{ij} \neq (S^n_{ij})^{-1}$ almost surely - and anisotropic. However, given the ergodicity of the Poisson-Voronoi mosaic, it can be shown from the variational principles (e.g., Huet, 1990; Ostoja-Starzewski & Schulte, 1996), that the ensemble averages of these two tensors provide, with the increasing scale δ, an ever tighter pair of bounds on $\boldsymbol{C}^{eff}$ (on a system of partitions)

$$\boldsymbol{C}^R \equiv \langle \boldsymbol{S}^n_1 \rangle^{-1} \leq \langle \boldsymbol{S}^n_{\delta'} \rangle^{-1} \leq \langle \boldsymbol{S}^n_\delta \rangle^{-1} \leq \boldsymbol{C}^{eff} \leq \langle \boldsymbol{C}^e_\delta \rangle \leq \langle \boldsymbol{C}^e_{\delta'} \rangle \leq \langle \boldsymbol{C}^e_1 \rangle \equiv \boldsymbol{C}^V_1 \qquad \forall \delta' < \delta \tag{2.6}$$

The order relation employed in (2.6) means that $t \cdot \boldsymbol{B} \cdot t \leq t \cdot \boldsymbol{A} \cdot t$ for any vector $t \neq 0$ and two second rank tensors $\boldsymbol{A}$ and $\boldsymbol{B}$. The resulting hierarchy of bounds is illustrated in Fig. 3 for contrast α = 1,000 of the microstructure shown in Fig. 2.

A prescription for the existence of the RVE (Hill, 1963) is that the relations between volume average stress and strain become the same in the $\delta \to \infty$ limit regardless of which one of these two

conditions has been used. This is the scale on which a deterministic C^{eff} is valid. Below the $\delta \to \infty$ limit, at every point $\underset{\sim}{x}$ in $\mathbf{B}(\omega)$, we have two tensors $C^e_\delta(\underset{\sim}{x}, \omega)$ and $S^n_\delta(\underset{\sim}{x}, \omega)$. Therefore, the random medium $\boldsymbol{B}$ may be described by two random tensor fields, which are parametrized by the mesoscale δ

$$\left\{C^e_\delta(\underset{\sim}{x}, \omega);\omega \in \Omega\right\} \qquad \left\{S^n_\delta(\underset{\sim}{x}, \omega);\omega \in \Omega\right\} \tag{2.7}$$

The scale dependence of average traces of both tensors follows, with excellent accuracy, for contrasts α = 10, 10^2, 10^3, and 10^4, the laws first found for planar Bernoulli lattices (Ostoja-Starzewski & Schulte, 1996)

$$\begin{aligned} \langle C^e_\delta \rangle &= a_0 + a_1 \exp\left(a_2 \delta^{-a_3 \alpha}\right) \\ \langle S^n_\delta \rangle^{-1} &= b_0 + b_1 \exp\left(b_2 \delta^{-b_3 \alpha}\right) \end{aligned} \tag{2.8}$$

(b) Probability distributions and correlation structure of mesoscale random fields

The probability densities of half-traces C^e_δ involved in the hierarchy (2.6) are shown in terms of their histograms in Fig. 3. Note the expected convergence of ensemble-averaged half-traces of C^e_δ and S^n_δ to a causal distribution with δ going to infinity - this is the classical, not practically attainable, RVE limit. The computations involved 1024 (= 32×32), 256 (= 16×16), 64 (= 8×8), and 16 (= 4×4) samples for window sizes δ = 10, 20, 40 and 80 employed in this figure; the numbers in brackets show the subdivisions of the square domain of Fig. 2 into $n \times n$ windows. The same samples allow an assessment of the statistics of radius R of the corresponding Mohr's circles of C^e_δ and S^n_δ. While the half-traces of these tensors display a nonsymmetrical character, their radii R have a much stronger skewness. However, a quick check

of the numbers shows that their coefficients of variation are found to be practically independent of the window size δ - they equal about 0.55 and 0.6 for $\boldsymbol{C}_\delta^e$ and $\boldsymbol{S}_\delta^e$, respectively. In fact, this striking feature has been established for other volume fractions (Ostoja-Starzewski, 1998b) as well as for microstructures of inclusion-matrix composite type with circular and needle-type inclusions of moderate aspect ratio (Ostoja-Starzewski, 1998c). Clearly, the mesoscale random fields are non-Gaussian, and we have found the Beta probability distribution to provide the most satisfactory and universal fits for this as well as other types of two-phase composites over a wide range of contrasts and mesoscales.

Application of micromechanics in a stochastic finite element method requires, besides the specification of one-point statistics of mesoscale moduli, a specification of their spatial correlations, so as to allow a rapid assignment of properties to all the elements given their relative spatial locations. That is, if we consider the random field $\boldsymbol{C}$, which stands either for $\boldsymbol{C}_\delta^e$ and $\boldsymbol{S}_\delta^n$, we should have some prescriptions for autocorrelations of its three components as well as their three crosscorrelations. Its spatial structure is described, to second order, by a *correlation coefficient*

$$\rho_{C_{ij}C_{kl}}(\underset{\sim}{x}, \underset{\sim}{x}') = \frac{\langle C_{ij}(\underset{\sim}{x})C_{kl}(\underset{\sim}{x}')\rangle - \langle C_{ij}(\underset{\sim}{x})\rangle\langle C_{kl}(\underset{\sim}{x}')\rangle}{\sigma_{C_{ij}}(\underset{\sim}{x})\sigma_{C_{kl}}(\underset{\sim}{x}')} \tag{2.10}$$

where all C_{ij} and C_{kl} stand for either C_{ij}^e and C_{kl}^e or S_{ij}^n and S_{kl}^n, while σ's are standard deviations of the indicated quantities. For a composite having stationary statistics of its properties, the random field $\boldsymbol{C}(\underset{\sim}{x})$ is wide-sense stationary, i.e.

$$\rho_{C_{ij}C_{kl}}(\underset{\sim}{x}, \underset{\sim}{x}') = \rho_{C_{ij}C_{kl}}(\underset{\sim}{r}) \qquad \underset{\sim}{r} = \underset{\sim}{x} - \underset{\sim}{x}' \tag{2.11}$$

When $\underset{\sim}{r} = \underset{\sim}{0}$, the latter quantity becomes a one-point correlation coefficient, written simply as $\rho_{C_{ij}C_{kl}}$. First. let us consider the cross-correlation between the C_{11} or C_{22} component and the C_{12} component of $\boldsymbol{C}_\delta^e$. We note that $\langle C_{11}C_{12}\rangle$ is either positive or negative depending on the actual orientation θ of the coordinate system x_1, x_2 with respect to the principal axes of $\boldsymbol{C}_\delta^e$.

However, since the probability density of θ is symmetric about zero for the isotropic statistics of the microstructure, $\rho_{C_{11}C_{12}} = \rho_{C_{22}C_{12}} = 0$. The same holds for the $\boldsymbol{S}_{\delta}^{n}$ tensor.

Next, in Fig. 4 we display the cross-correlations between C_{11}^{e} and C_{22}^{e} as well as S_{11}^{n} and S_{22}^{n} over the range of δ from 5 through 80. They are computed for the microstructure of Fig. 2. We observe that the spatial correlations between the mesoscale properties tend to zero with the window size increasing to infinity. The same type of result holds for two-point correlations.

A natural question arises here: is the $\boldsymbol{C}$ field isotropic in terms of its correlation function? Our computations, based on cross-correlating a window placed at $\underset{\sim}{x}$ with a window fixed at the origin of the coordinate system, indicate that $\boldsymbol{C}$ is a *quasi-isotropic* random field. In terms of a specific component of $\boldsymbol{C}$, say C_{ij}, this means that the equality $|\underset{\sim}{r}| = ||\underset{\sim}{s}||$ implies

$$\rho_{C_{ij}C_{kl}}(\underset{\sim}{r}) = \rho_{C_{ij}C_{kl}}(\underset{\sim}{s}) \tag{2.12}$$

where ρ is the autocorrelation function of C_{ij}, and $\underset{\sim}{s}$ is given by an invertible transformation

$$\underset{\sim}{s} = T(\underset{\sim}{r}) = [T_1(\underset{\sim}{r}), T_2(\underset{\sim}{r})] \qquad \underset{\sim}{r} = (r_1, r_2) \tag{2.13}$$

of $\boldsymbol{R}^2$ into $\boldsymbol{R}^2$. Here $|\underset{\sim}{r}|$ denotes a norm in $\boldsymbol{R}^2$, and $||\underset{\sim}{s}||$ a norm in $\boldsymbol{R}^2$ after the transformation.

Finally, we note that, the inherent independence property of the Poisson point placement process underlying the Voronoi mosaic precludes the correlations from being long range such as typically assumed through exponential correlation functions in the SFE literature. The above model may be applied to auto- and cross-correlations between all the components of $\boldsymbol{C}$; see (Ostoja-Starzewski, 1998a) for details on pixel systems and disk-matrix composites.

3. Window as a mesoscale finite element and macroscopic response

Let us now consider torsion of a bar of square cross section having in its cross section a two-phase microstructure of over one hundred thousand grains aligned with the bar's axis, Fig. 2. Thus, the macroscopic boundary value problem of interest to us is of the following form

$$\begin{aligned} \nabla \cdot [\boldsymbol{C}(\omega)\nabla\phi] + f &= 0 \qquad in \qquad \mathbf{B} \\ \phi &= 0 \qquad on \qquad \partial\mathbf{B} \end{aligned} \tag{3.1}$$

where ϕ is a stress function (Ostoja-Starzewski & Wang, 1998). Here $\boldsymbol{C}(\omega)$ corresponds to one particular realization $\mathbf{B}(\omega)$ of the random medium $\boldsymbol{B}$, so that the problem is entirely deterministic. The lower and upper bounds on global response are obtained, respectively, from two dual energy principles: a minimum potential energy principle

$$\inf_{\phi \in H_0^1(V)} \frac{1}{2}\int_V \underline{\eta}^T \boldsymbol{C}\underline{\eta}\, dV - \int_V f\phi\, dV \tag{3.2}$$

and, a minimum complementary energy principle

$$\inf \frac{1}{2}\int_V \underline{\xi}^T \boldsymbol{S}\underline{\xi}\, dV \qquad \forall \underline{\xi} \in \hat{H} = \left\{ \underline{\xi} \in (L_2(V))^2 \,\middle|\, \qquad \nabla \cdot \underline{\xi} + f = 0 \right\} \tag{3.3}$$

Here $\boldsymbol{C}$ and $\boldsymbol{S}$ are the stiffness and compliance tensors, while $\underline{\eta}$ and $\underline{\xi}$ stand for $\nabla\phi$ and $\boldsymbol{C}\underline{\eta}$, respectively.

Both energy principles ensure a monotonic convergence of the lower and upper bounds of the energy norm from below and above, respectively, in terms of the energy norm

$$\|\phi\|_E = \frac{1}{2}\int_V \underline{\eta}^T \boldsymbol{C}\underline{\eta}\, dV \tag{3.4}$$

provided we have a homogeneous material, e.g. (Brezzi & Fortin, 1991). This is shown in Fig. 5(a) as a function of the increasing finite element mesh resolutions: 4×4, 8×8, 16×16, 32×32, and 64×64; they correspond to $\delta \cong 5$, 10. 20, 40, and 81. Clearly, both bounds tend to coincide as the mesh becomes infinitesimally fine - this is the classical finite element limit.

Now, for a heterogeneous material, the effective stiffness tensor on mesoscales is nonunique, so that we need to exercise care in the interpretation of fields $\boldsymbol{C}$ and $\boldsymbol{S}$ in (3.2) and (3.3). Consid-

ering the fact that (3.2) is set up in displacements, $\boldsymbol{C}$ determined from displacement boundary condition (2.4) - i.e., $\boldsymbol{C}_\delta^e$ - should enter this principle. On the other hand, given the fact that (3.3) is set up in stresses, the effective compliances from natural boundary condition (2.5) - i.e., $\boldsymbol{S}_\delta^n$ - should be used as input to minimum complementary energy formulation. Since $\boldsymbol{C}_\delta^e$ or $\boldsymbol{S}_\delta^n$ are bounds on the possible Hooke's Law, both finite element methods provide bounds on the global, macroscopic response for given choice of δ.

Figure 5(a) indicates that, in the case of a homogeneous material, the finer is the mesh - i.e., the smaller is the mesoscale δ - the closer are both estimates of the global response. However, in the case of a heterogeneous material, there exists an opposing trend according to the hierarchy (2.6) and scaling laws (2.8). Thus we observe a competition of two opposing trends:

i) the global responses, computed by (3.2) and (3.3), tend to converge as δ decreases;

ii) the mesoscale responses, serving as input to (i), computed from the essential and natural boundary conditions ((2.4) and (2.5)), tend to diverge as δ decreases.

The results of this competition are shown in terms of the energy norm (3.4), as a function of the increasing finite element resolution, for three contrasts α = 10, 100, 1000 in Figs. 5b), c) and d). Fig. 5. Case d) is the one whose mesoscale statistics were displayed in Figs. 3 and 4. In the case b) of the relatively weak contrast (α = 10) an optimal finite element mesh size, or mesoscale δ_{opt}, can clearly be seen - it gives the closest upper and lower bounds. As the contrast increases - cases c) and d) - the bounds diverge further away from one another and only the crudest meshing of the entire domain provides a relatively useful estimate of the global response.

Our methodology employing mesoscale finite elements is checked by a comparison to the response of the same material without any approximating mesoscale finite element mesh - it presents an absolute and best available, albeit very costly, reference solution. Thus, in all four cases

of Fig. 5 a computational micromechanics solution directly taking into account the entire microstructure of 104,858 black and white cells, without any approximating mesoscale finite elements, is also shown. It is seen that these solutions always fall between the bounds based on the mesoscale moduli.

Finally, we have considered using a homogenization method, which relies on the concept of a periodic unit cell, e.g (Sanchez-Palencia & Zaoui, 1987; Mei *et al*, 1996). However, for our microstructure at the percolation point (Fig. 2), a periodic cell does not exist - whether on the scale of a single Voronoi grain or for a number of grains (e.g. Cruz *et al*, 1995). Yet another idea was to try a prescription for macroscopic effective moduli according to the random chessboard formula $C^{eff} = [C^{(1)}C^{(2)}]^{1/2}$, and then to use it as input for a finite element solution according to (3.2) and (3.3). Of course, as the mesh got finer, both schemes were converging just like the plots in Fig. 5a), but the energy norm (3.4) was deviating from the computational micromechanics results in Fig. 5b)-d), and the stronger was the contrast, the stronger was the deviation.

4. Conclusions

(a) The effective moduli on the mesoscale are almost surely non-unique, and anisotropic; they converge as the window tends to infinity. Statistics of these moduli are non-Gaussian; second invariants are highly skewed, but their coefficients of variation are practically constant.

(b) The mesoscale window is identified as a mesoscale finite element of the global finite element mesh. Mesoscale moduli derived from essential and natural boundary conditions provide input to global finite element solutions based on minimum potential energy and minimum complementary energy formulations, respectively. These solutions result in bounds on global response.

(c) With the demonstration of the method for a single realization of a random microstructure, it is a rather simple matter to generalize it to an ensemble response. This would involve a generation of realizations of random fields of mesoscale moduli C^e_δ or S^n_δ for several δ's based on the

statistics such as those presented in Section 2 (Figs. 3 and 4). The second step would consist of a formulation of global stiffness and flexibility matrices from these moduli. Finally, the third step would involve a solution of two finite element problems, for all the scales δ and all the realizations ω, for bounds on global stochastic response.

Acknowledgment

This research was supported by the National Science Foundation under grant CMS-9713764.

References

Benaroya, H. & Rehak, M. 1988 Finite element methods in probabilistic structural analysis: a selective review. *Appl. Mech. Rev.* **41**(5), 201-213.

Brezzi, F. & Fortin, M. 1991 *Mixed and Hybrid Finite Element Methods*, Springer-Verlag.

Cruz, M.E., Ghaddar, C.K. & Patera, A.T. 1995 A variational-bound nip-element method for geometrically stiff problems: application to thermal composites and porous media. *Proc. R. Soc. Lond, Ser. A* **449**, 93-122.

Ditlevsen, O. 1996 Dimension reduction and discretization in stochastic problems by regression method, in *Mathematical Models for Structural Reliability Analysis*, 51-138, CRC Press.

Ghanem, R. and Spanos, P.D. 1991 *Stochastic finite elements: a spectral approach*, Springer-Verlag, Berlin.

Hill, R. 1963 Elastic properties of reinforced solids: some theoretical principles. *J. Mech. Phys. Solids* **11**, 357-372.

Huet, C. 1990 Application of variational concepts to size effects in elastic heterogeneous bodies. *J. Mech. Phys. Solids* **38**, 813-841.

Mei, C.C., Auriault, J.-L. & Ng, C. 1996 Some applications of the homogenization theory. *Adv. Appl. Mech.* **32**, 277-348.

Ostoja-Starzewski, M. & Schulte, J. 1996 Bounding of effective thermal conductivities of multiscale materials by essential and natural boundary conditions. *Phys. Rev. B* **54**, 278-285.

Ostoja-Starzewski, M. 1998a Random field models of heterogeneous materials. *Intl. J. Solids Struct.*, **35**, 2429-2455.

Ostoja-Starzewski, M. 1998b Random field models and scaling laws of heterogeneous media. *Arch. Mech.*, **50**(3), 549-558.

Ostoja-Starzewski, M. 1998c Scaling effects in materials with random distributions of needles or cracks. *Mech. Mater.* submitted.

Ostoja-Starzewski, M. & X. Wang, X. 1998 Stochastic finite elements as a bridge between random material microstructure and global response. *Comp. Meth. Appl. Mech. Eng.*, in press.

Sanchez-Palencia, E. & Zaoui, A. (eds.) 1987 *Homogenization Techniques for Composite Media*, Lecture Notes in Physics **272**.

Werner, E., Siegmund, T., Weinhandl, H. & Fischer, F.D. 1994 Properties of random polycrystalline two-phase materials. *Appl. Mech. Rev.* **47**(1, Pt. 2), S231-S240.

List of Figures

Fig. 1 A macroscopic body with a mesoscale window (or finite element) of size L, in which a microstructure of grain size d is shown.

Fig. 2 A two-phase material with a Voronoi mosaic microgeometry of a total 104,858 black and white cells, at volume fraction 50% each.

Fig. 3 Hierarchies of average moduli $\langle S^n_\delta \rangle^{-1}$ and $\langle C^e_\delta \rangle$, for increasing window size $\delta \cong 10, 20,$ 40, and 80, of the two-phase microstructure of Fig. 2, with $C^{(1)} = 1$ and $C^{(2)} = 2$ (i.e., contrast $\alpha = 10$).

Fig. 4 Cross-correlations of C^e_{11} with C^e_{22} and S^n_{11} with S^n_{22} as a functions of the increasing window size $\delta \cong 5, 10, 20, 40,$ and 80. Fluctuations are due to the finite sample size, but the trend is evident.

Fig. 5 Behavior of the energy norm (3.4) with respect to a sequence of self-accommodating finite element meshes, in terms of the increasing finite element resolution, on: (a) a homogeneous material domain contrast $\alpha = 1$, and (b) a heterogeneous domain of Fig. 2 for contrast $\alpha = 10$, (c) the same domain for $\alpha = 100$, and (d) the same domain for $\alpha = 1{,}000$. In (b), (c), and (d) a computational micromechanics solution taking directly into account the entire microstructure of 104,858 black and white cells is also shown.

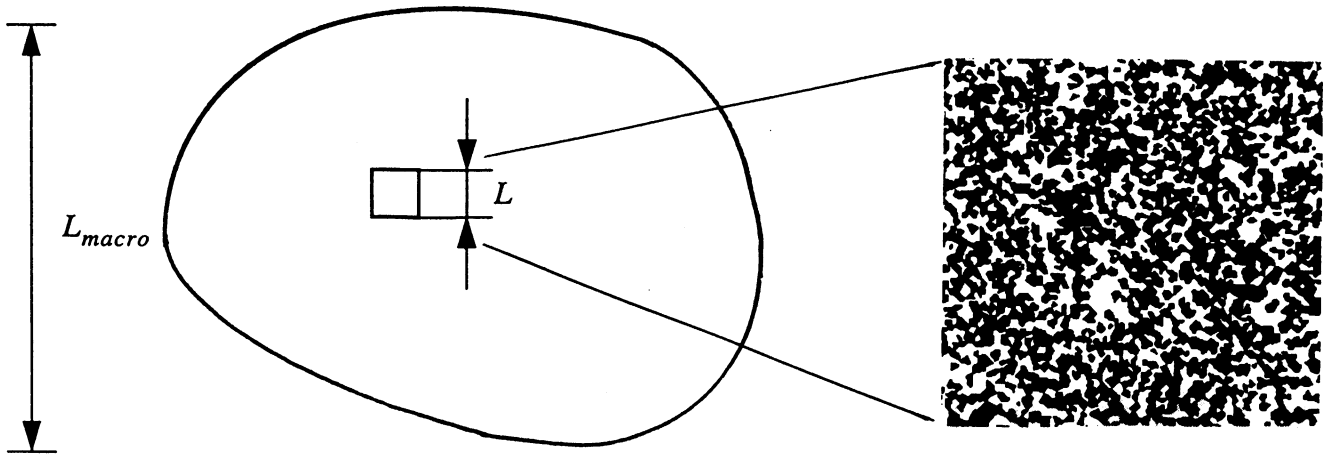

Fig. 1

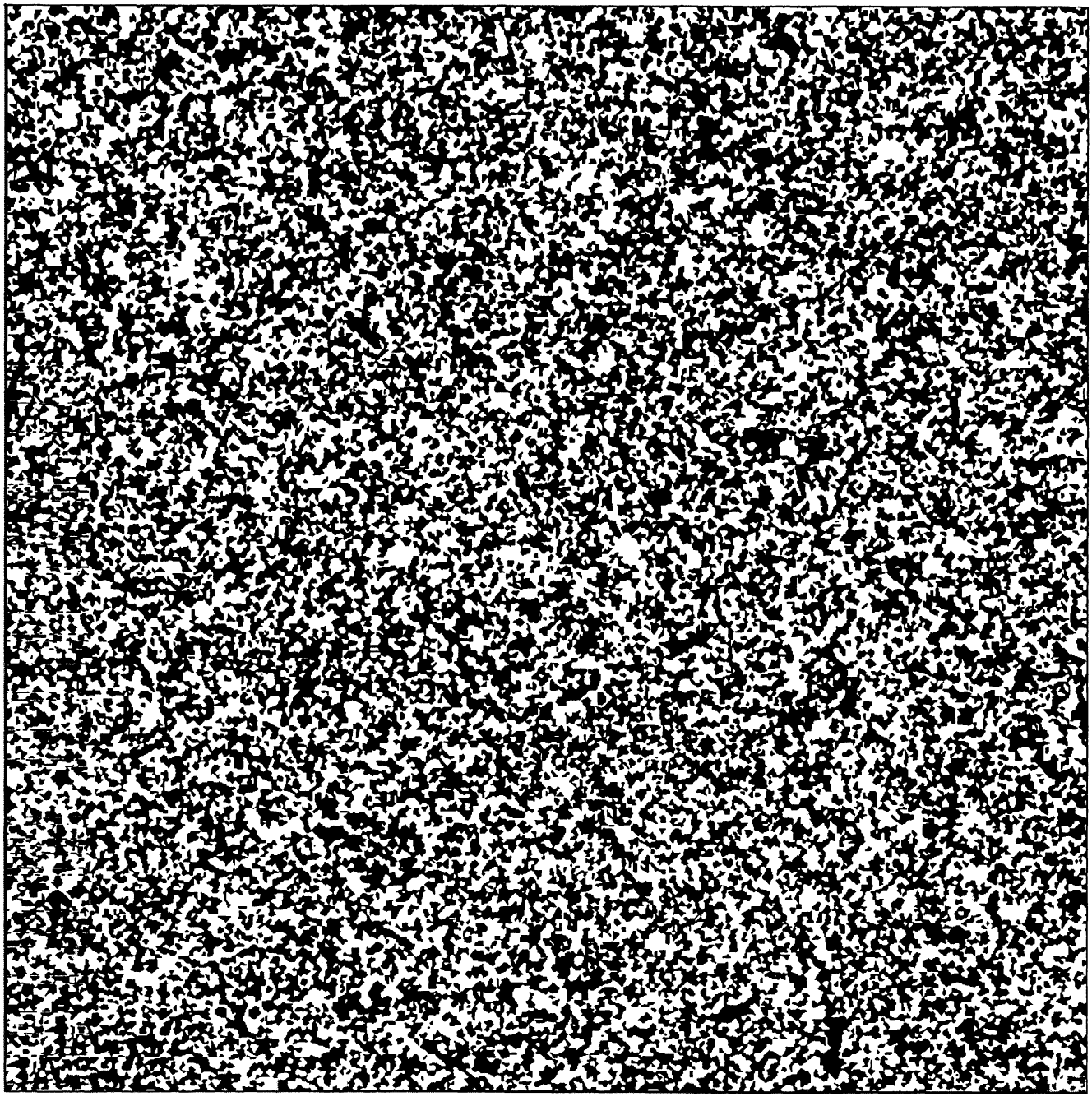

Fig. 2

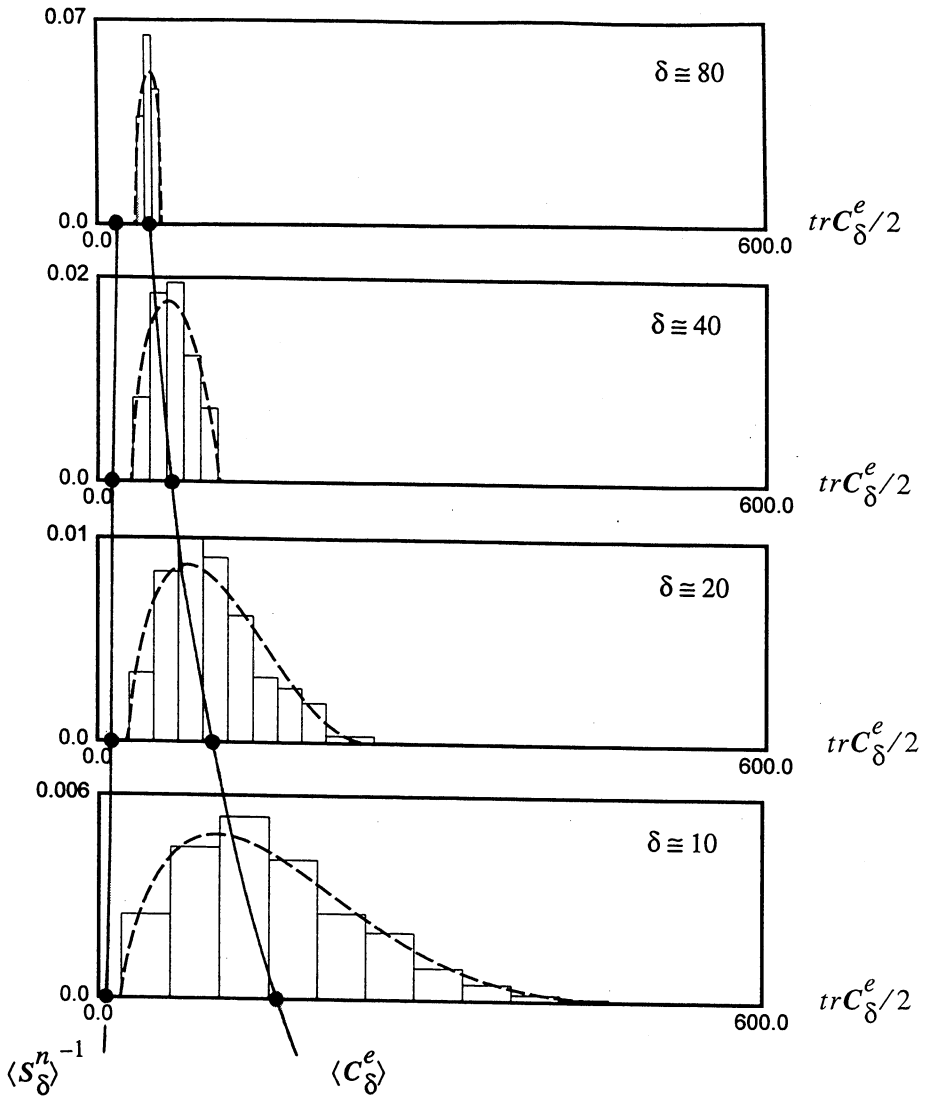
0.07
δ ≅ 80
0.0
0.0
600.0
$trC_\delta^e/2$
0.02
δ ≅ 40
0.0
0.0
600.0
$trC_\delta^e/2$
0.01
δ ≅ 20
0.0
0.0
600.0
$trC_\delta^e/2$
0.006
δ ≅ 10
0.0
0.0
600.0
$trC_\delta^e/2$
$\langle s_\delta^n \rangle^{-1}$
$\langle C_\delta^e \rangle$

Fig. 3

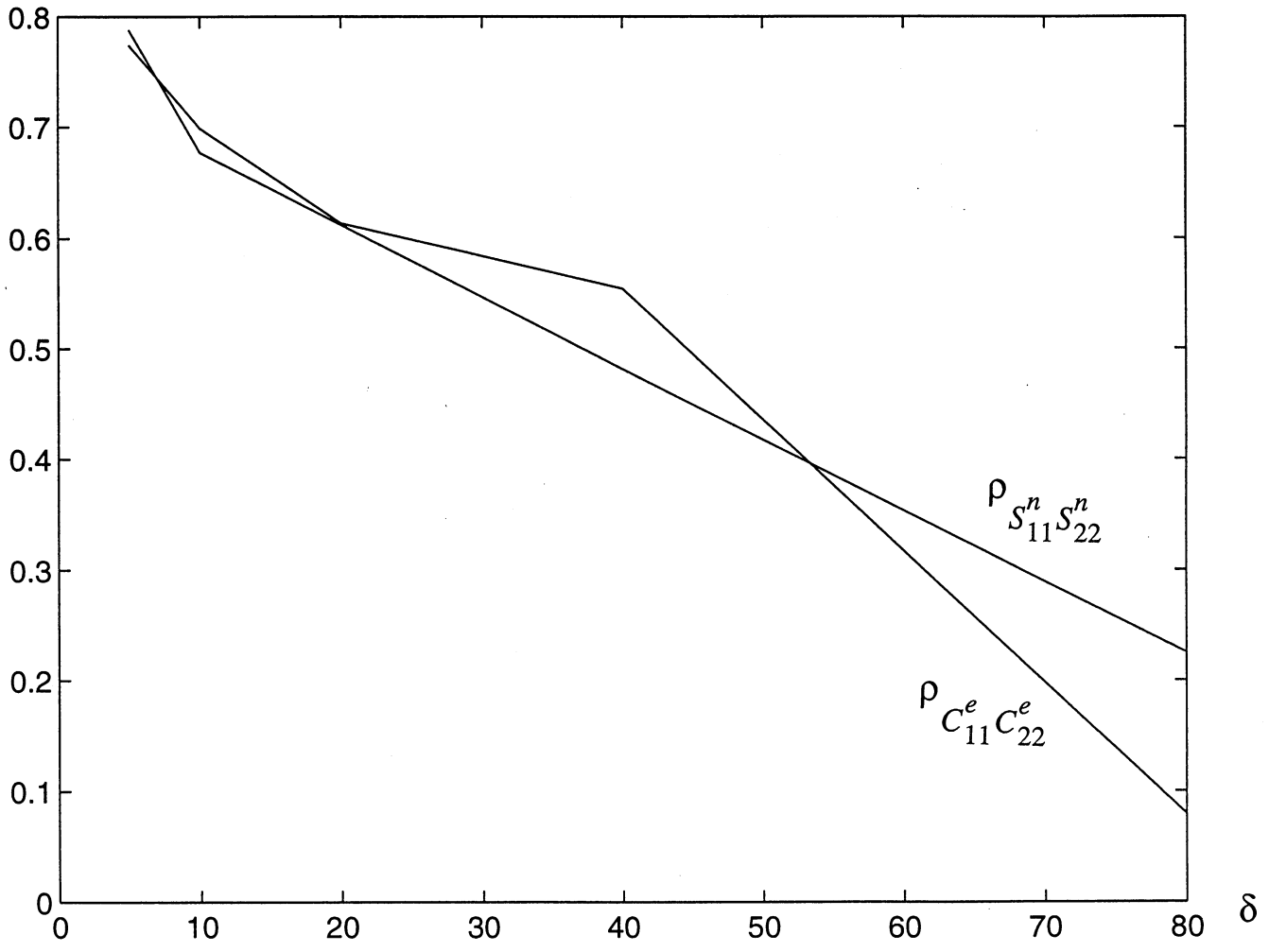
0.8
0.7
0.6
0.5
0.4
0.3
0.2
0.1
0
0
10
20
30
40
50
60
70
80
δ
$\rho_{S_{11}^n S_{22}^n}$
$\rho_{C_{11}^e C_{22}^e}$

Fig. 4

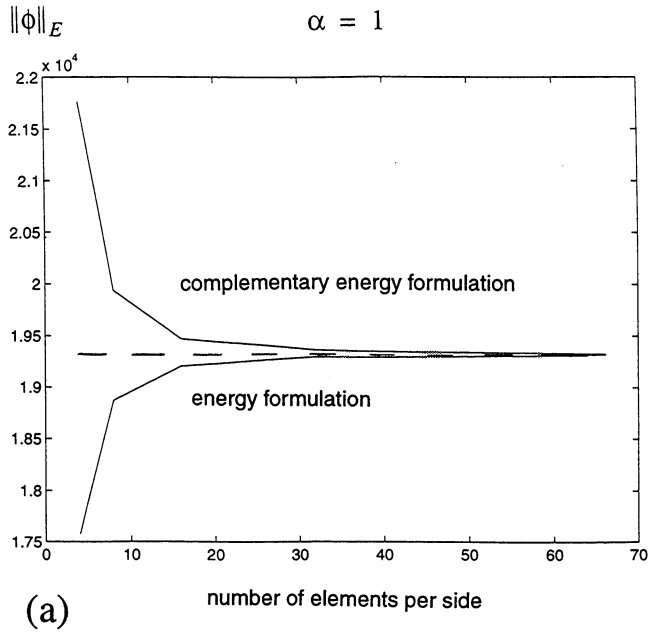
$\|\phi\|_E$
$\alpha = 1$
x 10^4
2.2
2.15
2.1
2.05
2
1.95
1.9
1.85
1.8
1.75
complementary energy formulation
energy formulation
0
10
20
30
40
50
60
70
number of elements per side

(a)

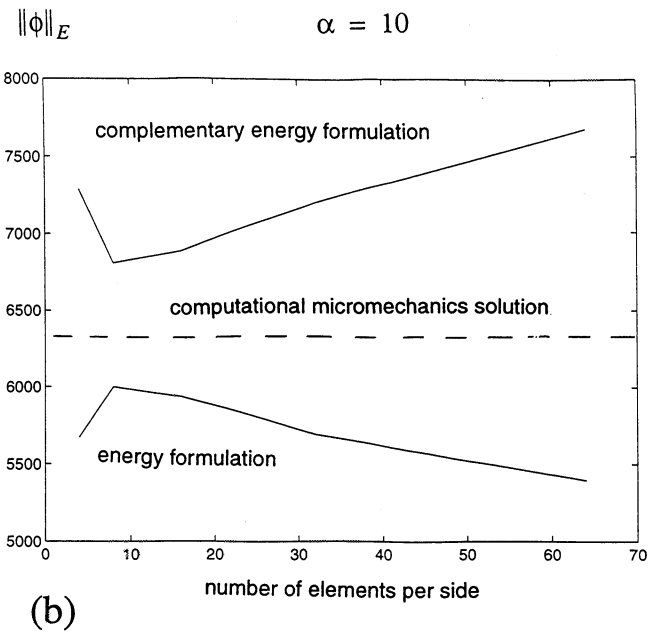
$\|\phi\|_E$
$\alpha = 10$
8000
7500
7000
6500
6000
5500
5000
complementary energy formulation
computational micromechanics solution
energy formulation
0
10
20
30
40
50
60
70
number of elements per side

(b)

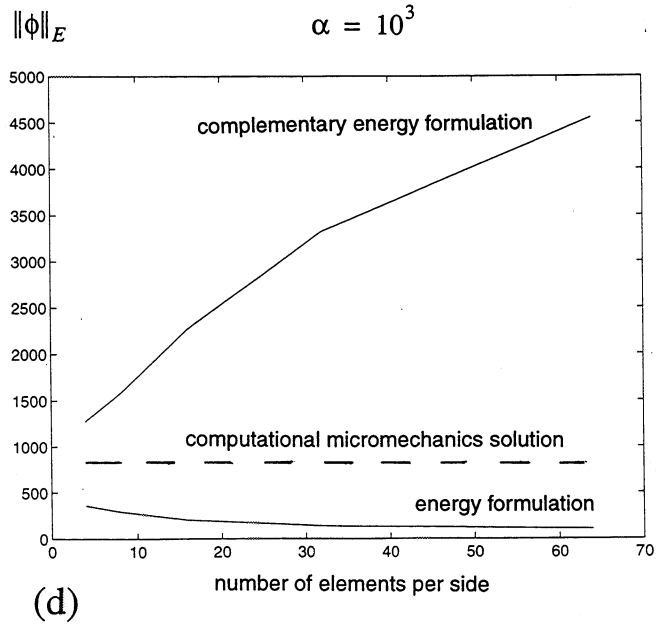
$\|\phi\|_E$
$\alpha = 10^3$
5000
4500
4000
3500
3000
2500
2000
1500
1000
500
0
complementary energy formulation
computational micromechanics solution
energy formulation
0
10
20
30
40
50
60
70
number of elements per side

(d)

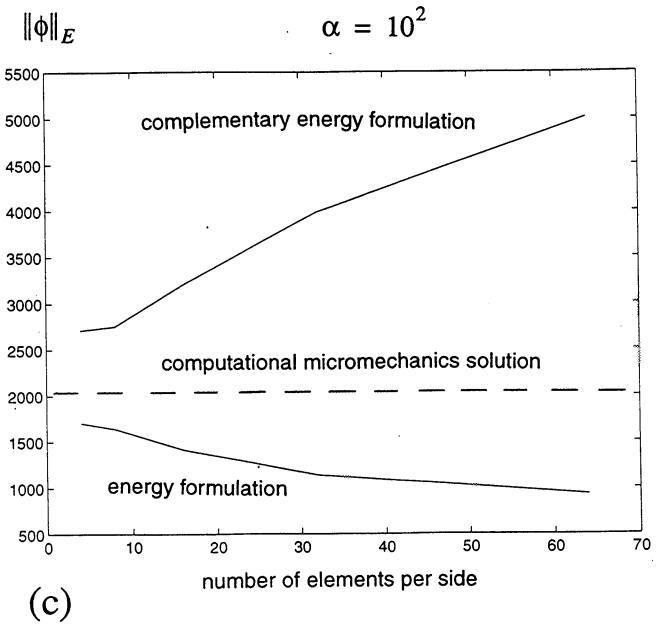
$\|\phi\|_E$
$\alpha = 10^2$
5500
5000
4500
4000
3500
3000
2500
2000
1500
1000
500
complementary energy formulation
computational micromechanics solution
energy formulation
0
10
20
30
40
50
60
70
number of elements per side

(c)

Fig. 5